Simulation and Control of a Methanol-To-Olefins (MTO) Laboratory Fixed-Bed Reactor

Farzi, Ali**+; Jomea, Mohammad Javad

Faculty of Chemical and Petroleum Engineering, University of Tabriz, Tabriz, I.R. IRAN

ABSTRACT: *In this research, modeling, simulation and control of a methanol-to-olefins laboratory fixed-bed reactor with electrical resistance furnace has been investigated in both steady-state and dynamic conditions. The reactor was modeled as a one-dimensional pseudo-homogeneous system. Then, the reactor was simulated at steady-state conditions and the effect of different parameters including inlet flow rate, inlet temperature and electrical resistance temperature on reactor performance was studied. Results showed that the most effective parameter is electrical resistance temperature. Thus, it was selected as manipulating variable for controlling product quality. In the next step, dynamic simulation of the process was performed and the effect of different disturbances on the dynamic behavior of the reactor was assessed. Finally, PID and Neural Network Model Predictive (NNMP) controllers were utilized for process control, and their performances were compared to each other. The response of the control system to different disturbances and set point changes showed that both PID and NNMP control systems can maintain the process at the desired conditions. PID controller had smaller rise time and no offset compared to NNMP controller while NNMP controller had smaller overshoot.*

KEYWORDS: *Methanol-To-Olefins (MTO); Dynamic simulation; Electrical resistance furnace; Artificial Neural Network (ANN); Neural Network Model Predictive Control (NNMPC).*

INTRODUCTION

Light olefins including ethylene and propylene are very important intermediate components in petrochemical industries. Global demand for ethylene and propylene was significantly high in recent years. This growth rate of demand for light olefins, as well as significant increase of crude oil price, has brought about more attention to the direct production technologies, especially from non-oil resources [1].

Recently methanol has gained more attention for this purpose. Performed schedules for significant increase in global production capacity of methanol, introduce it as a non-oil resource for production of light olefins. Process of converting methanol to hydrocarbons recently has gained attention as a powerful method to convert coal into gasoline. In fact, by the aid of this new technology, almost anything can be made from coal or natural gas which can be made from crude oil. For coal-rich countries, e.g. China, developing coal-based olefins industry is of great importance for their national economy [2.3].

MTO process was first discovered in 1970s during development of Mobil's Methanol-To-Gasoline (MTG)

* *To whom correspondence should be addressed.*
\+ *E-mail: a-farzi@tabrizu.ac.ir*
1021-9986/2017/2/175-190 16/$/6.60

process over a medium-pore zeolite of ZSM-5 class [4]. Considerable efforts were subsequently assigned to the MTO process and significant advancements have been achieved during the past years which cover various aspects of the process, such as catalyst evaluation [5-8], reaction mechanism [9-12], kinetic modeling [13-21], and catalyst deactivation [22-27]. This process is also attractive because of its low CO_2 emission [28].

The kinetic models for this process can be grouped into two main classes:

(a) *Lumped models*, which are an agreement between simplicity and representation of the process reality. It was found in 1970s that the initial step of ether formation is much more rapid than the subsequent olefins forming step, and is essentially at equilibrium [29, 30]. Thus, the equilibrium oxygenate mixture can be treated as a single kinetic species. Based on these facts, *Voltz & Wise* developed a lumped kinetic model [31]. *Bos et al.* [13] presented a kinetic model for MTO process using SAPO-34 catalyst. This kinetic model involves 12 reactions where 10 reactions are first order and two others are second order. *Gayubo et al.* [14] modeled methanol to olefins process in a fixed bed reactor with SAPO-34 catalyst using kinetic model proposed by *Bos et al.* [13]. They proposed a kinetic model and studied the role of water on catalyst activity and selectivity [32]. *Chen & Reagan* found out that the oxygenate disappearance over ZSM-5 is autocatalytic [33]. Autocatalysis was supported by measurements obtained by *Chang et al.* who extended the model with some assumptions [34].

(b) *Detailed models*, that take into account individual reaction steps. *Park & Froment* developed a software tool to determine components involved in the reaction [15, 16]. *Mihail et al.* [19] developed a detailed kinetic model based on ZSM-5 catalyst which involves 53 reactions and 36 species including intermediates. *Kaarsholm et al.* [21] also developed a detailed kinetic model for reaction of methanol over ZSM-5 catalyst in a fluidized-bed reactor. In their work influence of water on kinetics was taken into account and kinetic parameters of the reactions were found using constrained optimization.

In general, the conversion of methanol to olefins reaction can be done in fixed or fluidized-bed reactors. Although, the fluidized-bed reactor has some advantages in exothermic reactions due to better heat transfer and temperature control, but relatively low methanol conversion with significant catalyst attrition, and also high investment for reactor scale up, are the main disadvantages [35]. Fixed-bed reactor is simple in construction and easily operable and is a primary type of reactor that must be considered and plays a very important role in chemical industry [36, 37].

Modeling and simulation of fluidized and fixed-bed reactors of MTO process have been performed for many industrial and pilot-scale reactors. *Schoenfelder et al.* [38] developed a reactor model of Circulating Fluidized Bed (CFB) for MTO process. A lumped kinetic model was incorporated into model equations. In their study, the kinetic experiments were carried out in a standard fixed-bed reactor instead of CFB. *Soundararajan et al.* [39] modeled MTO process at steady-state conditions using SAPO-34 catalyst within a CFB reactor and used kinetic model of *Bos et al.* [13] for process modeling. They performed their simulations at 450°C and atmospheric pressure and investigated the effect of coke content and exit geometry on olefins yield and found that optimum ethylene yield is 27.2 wt% with 5% coke on catalyst. *Alwahabi & Froment* [35] predicted yields and selectivities of products in fixed-bed reactors, either multi-tubular and quasi-isothermal or multi-bed adiabatic and also in fluidized bed reactors. *Zhuang et al.* [37] performed dynamic simulation of MTO process in a fixed-bed reactor using Fluent. The catalyst they used was SAPO-34. They investigated the effect of feed temperature, space velocity and water/methanol ratio on the reactor performance and found their optimum values. *Chang et al.* [40] used CFD model for simulation of MTO process in a fluidized-bed reactor. They investigated velocity profile, volume fraction and species concentrations in axial and radial directions of the reactor and the effect of coke deposition on methanol conversion [40]. Also *Lu et al.* [41] performed CFD simulation of MTO process in a fluidized-bed reactor. They integrated chemical reaction engineering model in order to speed up simulations. Both above-mentioned works extended the work of *Soundararajan et al.* [39] who modelled a circulating fluidized-bed reactor for MTO process on SAPO-34 catalyst.

Although few studies have been carried out on dynamic simulation of fixed-bed reactors, no significant work was found for control of MTO process in this type of reactors.

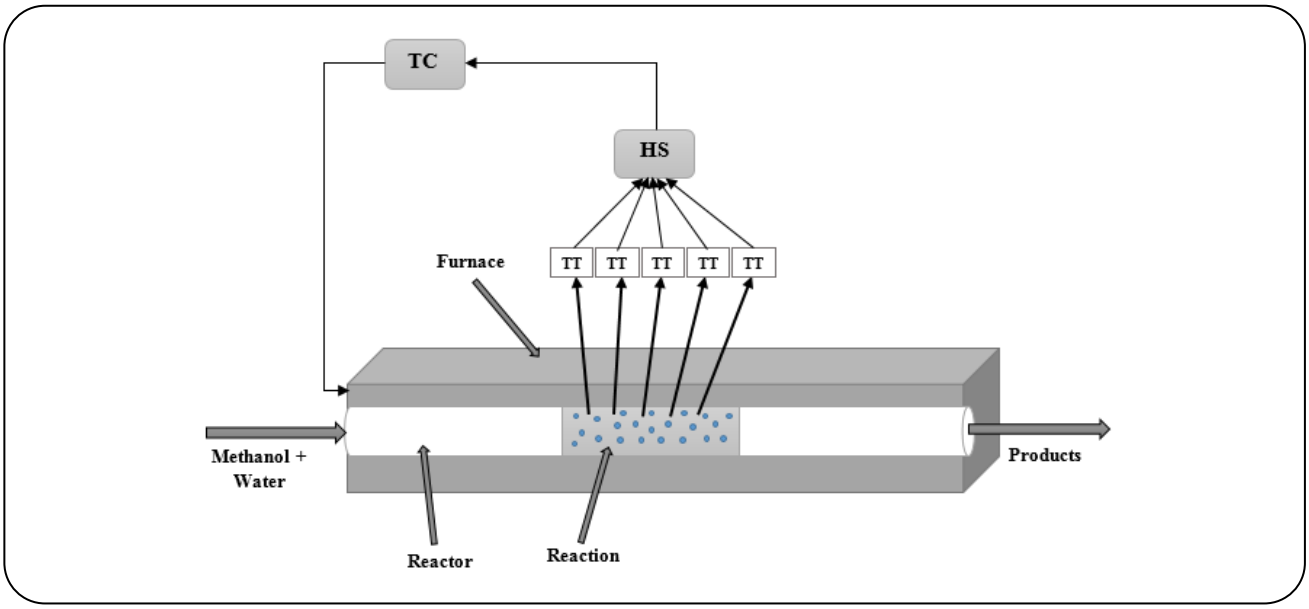

Fig. 1: Experimental reactor used for MTO process.

In this study, dynamics behaviour of MTO process in a fixed-bed reactor was investigated using mathematical modeling and simulation. Also, control of the process using classical and Artificial Neural Network (ANN)-based controllers and their performance has been assessed.

THEORITICAL SECTION

Reaction kinetics

The kinetic model used in this paper is the model of *Mihail et al.* [19] who proposed reaction path for the methanol conversion to hydrocarbons as below:

$$CH_3OH \underset{+H_2O}{\overset{-H_2O}{\rightleftharpoons}} CH_3OCH_3 \longrightarrow \qquad (1)$$

$$\text{Light olefins} \longrightarrow \begin{cases} \text{Paraffins} \\ \text{Aromatics} \end{cases}$$

As mentioned before, the model consists of 53 reactions in which 5 reactions are in equilibrium. Detailed reaction network is presented in Appendix A. All reactions are assumed to be elementary and their kinetic equations are represented in the following form [19].

$$R_j = k_j \prod_{i=1}^{m_s} C_i^{a_{ij}} \quad , \quad k_j = k_{j0} \exp\left(-E_j / RT\right), \qquad (2)$$

$$j = 1, 2, \ldots, m$$

All parameters are introduced in Symbols section. The most important species include methanol, water, ethylene and propylene.

Reactor model

Olefins production process studied in this research consists of a fixed bed reactor with electrical resistance furnace as illustrated in Fig. 1. The process involves injecting methanol as feed into a reactor with a glass tube that is electrically heated. Specifications of fixed-bed reactor are presented in Table 1 [19].

Using an adiabatic reactor causes a sharp increase in temperature of the reactor which can damage catalyst. On the other hand, if the temperature of the reactor is reduced below a specified value because of heat transfer to ambient, methanol conversion will not occur. Therefore, the temperature inside the reactor must be adjusted at an optimal level. For this reason, it is needed to place an electrical resistance around the reaction zone, to maintain the temperature about 50°C under the temperature inside the reactor, because the main reactions are highly exothermic. The catalyst used in this process is ZSM-5 with SiO_2/Al_2O_3 ratio of 24 [19].

Mathematical model

In this study, fixed-bed reactor was modeled as a one-dimensional, pseudo-homogeneous dynamic reactor. The following assumptions was made for process modeling:

1. The flow pattern through the reactor is assumed to be plug.

2. Axial diffusion and dispersion is assumed negligible with respect to bulk mass transfer.

Table 1: Specifications of fixed-bed reactor shown in Fig. 1.

Active Length (m)	0.1
Diameter (m)	0.02
Catalyst volume (m^3)	10^{-5}
Volume of inert material (m^3)	10^{-5}
Inlet pressure (Pa)	101325
Feed components	CH_3OH and/or H_2O

3. There is no radial temperature and concentration gradients, based on assumption 1.

4. Because catalyst particles are very small, the concentration and temperature variations within pores of particles can be neglected.

5. Effectiveness factor is assumed to be fixed at 1.

6. Gas phase is assumed to be ideal.

Based on the above assumptions component-mass and energy balance equations was obtained for the process which are presented as below:

Mass balance for component *i*:

$$\varepsilon\frac{\partial F_i}{\partial t}=-u\frac{\partial F_i}{\partial z}+(1-\varepsilon)u\eta r_i A,\qquad i=1,2,\ldots,m_s \tag{3}$$

where:

$$r_i=\sum_{j=1}^{m}\nu_{ij}R_j \tag{4}$$

Energy balance:

$$\left[\frac{\varepsilon}{uA}\sum_{i=1}^{m_s}F_i\left(C_{pi}^{ig}-R\right)+(1-\varepsilon)\rho_{cat.}C_{pcat.}\right]\frac{\partial T}{\partial t}= \tag{5}$$

$$\frac{4U}{d}\left(T_a-T\right)-\frac{1}{A}\sum_{i=1}^{m_s}F_iC_{pi}^{ig}\frac{\partial T}{\partial z}+\eta(1-\varepsilon)\sum_{j=1}^{m}R_j\left(-\Delta H_j\right)$$

37 partial differential equations were obtained from component mass and energy balances including intermediate species which must be solved simultaneously, to obtain profiles for concentrations of components and temperature through the bed at dynamic conditions.

Initial and boundary conditions for solving the equations are as below:

Boundary conditions:

$$F_i\Big|_{z=0,t}=F_{i0},\ T\Big|_{z=0,t}=T_0$$

Initial conditions:

$$F_i\Big|_{z,t=0}=F_i^{ss},\ T\Big|_{z,t=0}=T^{ss}$$

Overall heat transfer coefficient was calculated using the following equation [19]:

$$\frac{1}{U}=\frac{1}{K}+\frac{1}{(\alpha_{ra}+\alpha_{conv})\left(1+\frac{2\delta}{d}\right)} \tag{6}$$

Convective heat transfer coefficient, $\alpha_{conv.}$, was taken from the work of *Green & Perry* [42]. Radiative heat transfer coefficient, α_{ra}, was computed according to *Hottel & Sarofim* [43]. Conduction heat transfer coefficient of the outer wall, K, is given by Froment [44]:

$$\frac{1}{K}=\frac{d}{8\lambda_{eff}}+\frac{1}{\alpha_{W,eff}}+\frac{1}{\frac{\lambda_W}{\delta}.\frac{2R_M}{d}+\alpha_{ra}} \tag{7}$$

where R_M is defined as:

$$R_M=\frac{\delta}{\ln\left(1+\frac{2\delta}{d}\right)} \tag{8}$$

The effective radial conductivity of the bed and the effective wall heat transfer coefficients were computed according to [45-47].

Numerical Method

For solving the system of nonlinear partial differential equations obtained from dynamic modeling, method of lines was used. In this method time derivative is kept unchanged and partial differential equations are converted into a set of ordinary differential equations by applying finite differences method on derivatives with respect to spatial coordinate [48]. The number of obtained ordinary differential equations depends on the number of divisions applied on the reactor length.

Electrical Resistance Furnace model

When theoretical models are impractical or impossible to obtain, for example when the process is complex or there are many parameters in theoretical model, semi-empirical models of the process can be good alternative which are usually based on the open-loop response of the system. Table 2 shows the specifications of a laboratory electrical resistance furnace equipped with a temperature controller.

Fig. 2 shows the response of this system to a +50ºC

Table 2: Specifications of laboratory-scale electrical resistance furnace.

Maximum temperature of the furnace (K)	1073.15
Inside diameter (m)	0.06
Length (m)	0.3
Maximum power (kW)	1.5
Maximum intensity of the electric current (A)	7
Temperature Control System	PID

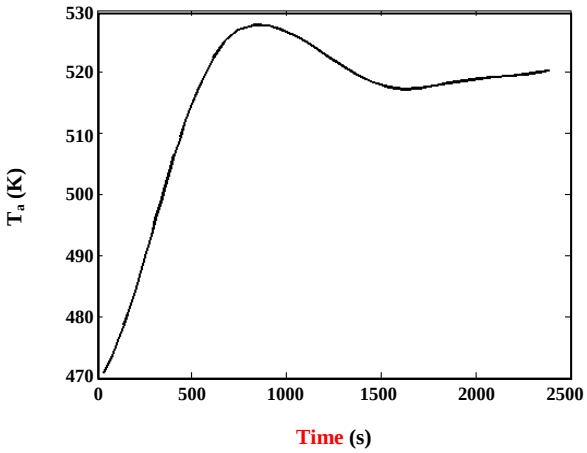

Fig. 2: Experimental response obtained for +50ºC step change in input temperature of electrical resistance furnace.

step change in its input. As can be seen, electrical resistance furnace acts as a second order system with delay.

$$G_{furnace} = \frac{T_a(s)}{T_{aref}(s)} = \frac{K_p e^{-\tau_d s}}{\tau^2 s^2 + 2\tau\zeta s + 1} \quad (9)$$

The parameters of the system were estimated based on the above system response and are given in Table 3.

Process control

For control of MTO process two types of controllers including PID and ANN-based controllers were used. Although PID controller is well-known for all researchers, but use of ANNs for process control is relatively a new area of research. ANNs are simplified models of biological neural networks and have learning capability like human. A feed-forward ANN consists of an input layer, one or more hidden layers consisting of neurons and one output layer whose number of neurons is equal to the number of network outputs. Each neuron applies an activation function on weighted sum of its inputs to generate its output [49, 50]. The schematic of a simple multi-layer feed-forward artificial neural network is shown in Fig. 3, where x_i is input variable to the i th neuron, $w_{i,j}$ represents weight between output of neuron i and input of neuron j, θ_k is weight of bias input to kth neuron, and O_k is network output from kth output neuron.

Training of an ANN means adjustment of all weights in the network by the aid of a training algorithm in such a way that for a specified set of input variables its outputs fit closely the desired outputs or targets of the system. After training, it can be used for the simulation of real system [49-50].

Feed-forward ANNs are statics systems and can only be used to model steady-state conditions. Because process control is inherently dynamic, they cannot be used directly and must be extended to include time changes of input and output variables of the system. Recurrent networks are another class of ANNs which are used for modeling and simulation of dynamic systems including process control. These networks can store values of their input and output variables at previous time steps in order to use at current time step for prediction of current outputs of the network. Training of these networks is more complex than feed-forward ANNs, but the basics are the same. Initially, different sets of inputs and outputs of real system at dynamic conditions are gathered and then they are used for training of the network [49, 51].

There are different types of recurrent networks which are used for process control. Among them one of the widely-used method is Neural Network Model Predictive Control (NNMPC) method. In this method, discrete-time process model is used to predict future behavior of the system, and an optimization algorithm is used to calculate the control input that optimizes future performance. The objective function is a weighted least squares function of outputs of processing system, set point and controller outputs which must be minimized subject to constraints such as maximum overshoot, rise time, etc. The optimization problem could be solved by classic optimization techniques, search methods, or evolutionary algorithms. The details of optimization problem can be found in [52].

Table 3: Calculated parameters for closed-loop electrical resistance furnace model (Eq. (9)).

K_p	τ (s)	ζ	τ_d (s)
1	225.6	0.517	25

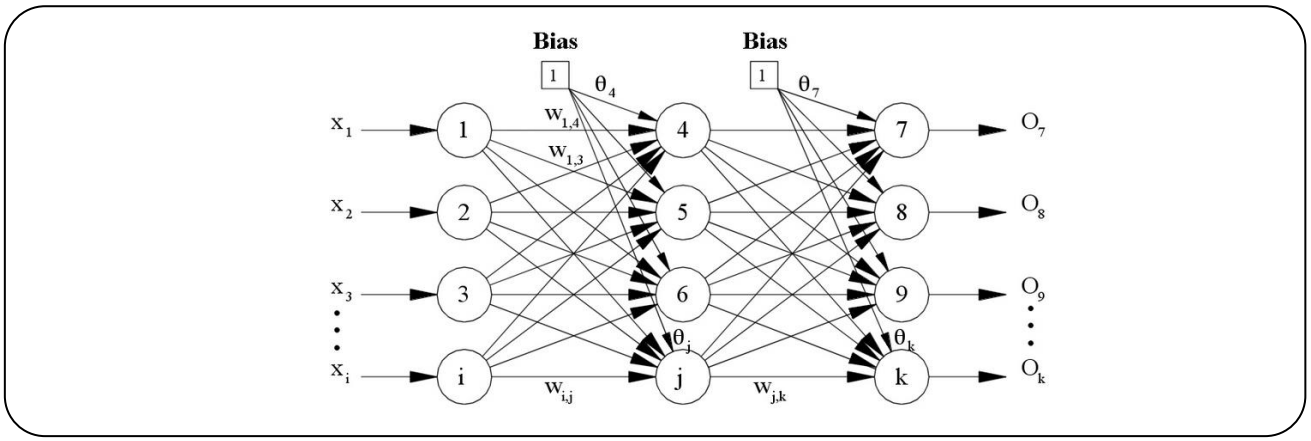

Fig. 3: Schematic of a multi-layer feed-forward ANN.

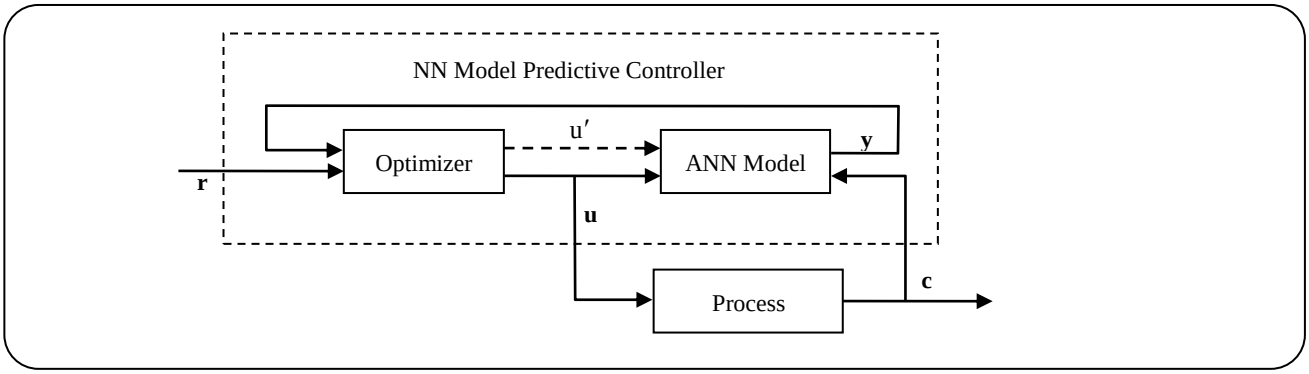

Fig. 4: Structure of NNMP control system used in this study.

The neural network is trained offline. Because of using an optimization algorithm for prediction of future input to the process it can control and reject disturbances with good speed and low overshoot [52-57]. In this work NNMP controller of MATLAB™ neural network toolbox was used. The structure of NNMP control system used in this study is shown in Fig. 4:

RESULTS AND DISCUSSION

Steady-state simulation

Before carrying out dynamic simulation, optimum initial conditions of the system must be obtained by solving model equations at steady-state conditions. For steady-state simulation, accumulation terms in mass and energy balance equations were set to zero. Then the resulting system of 37 ordinary differential equations was solved using a specific type of Runge-Kutta method for solving the system of stiff equations [58]. The results of steady-state simulation of MTO process are presented at below.

Effect of water content on reactor performance

To investigate the effect of water content on reactor performance, two tests were performed. In first test, pure methanol was injected into the reactor and product distribution along the reactor was obtained by simulation which is illustrated in Fig. 5. As can be seen, methanol concentration decreased through the reactor while concentrations of products increased. Di-methyl ether is an intermediate product and its concentration

Table 4: Operating conditions [19] and simulation results at steady-state conditions

Operating conditions	Run no. 1	Run no. 2
Mass flow-rate × 10^5 (kg/s)	0.274	0.293
Feed composition, CH_3OH+H_2O (wt%)	100 + 0	75 + 25
Feed Temperature (K)	650	650
Electrical resistance temperature (K)	610	610

	Run no. 1			Run no. 2		
Components (wt%)	EXP.	MODEL	Error	EXP.	MODEL	Error
H2O	53.14	52.17	1.83%	62.38	63.55	1.88%
C2H4	6.97	6.77	2.87%	5.68	5.22	8.10%
C3H6	5.16	2.7	47.68%	4.42	2.7	38.91%
C4H8	2.53	1.6	36.76%	2.19	1.5	31.51%
C5H10	0.52	0.32	38.46%	0.37	0.21	43.24%

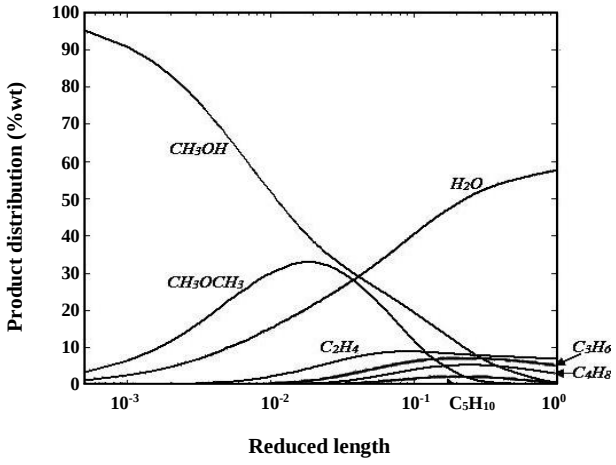

Fig. 5: Product distribution with inlet pure methanol.

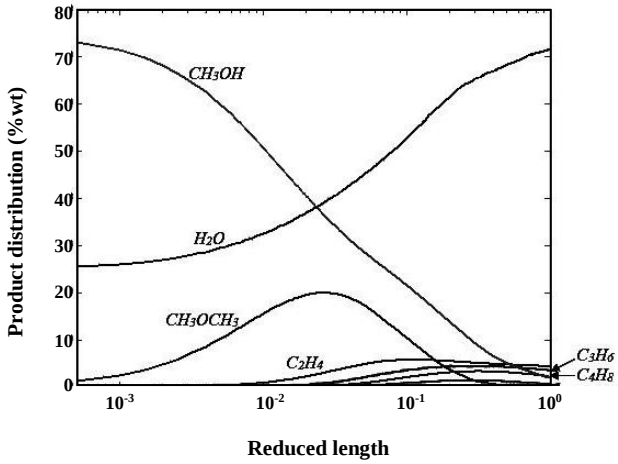

Fig. 6: Product distribution with inlet methanol (75 wt%) and water (25 wt%).

firstly increases and then decreases. In second test, methanol and water were injected together in order to observe the effect of adding water into inlet flow. Profiles of products distribution along the reactor obtained by simulation are shown in Fig. 6. By comparing the results of two tests it is evident that by adding water into inlet stream, light olefins concentration decreased slightly. Inlet water greatly influences temperature distribution and causes the temperature inside the reactor to decrease. Also, using water in inlet stream reduces coke formation on catalyst and prevents catalyst deactivation. Simulation and experimental results as well as percent error of simulation results for main components, are presented in Table 4. The results show an acceptable match and therefore the assumptions are appropriate.

Influence of water on temperature distribution within the reactor is shown in Fig. 7. As can be seen, temperature increases sharply at inlet of the reactor because the main reactions are highly exothermic and fast. Then, because of the start of endothermic reactions, temperature decreases. Temperature increase is lower in the case of adding water to inlet stream which is because

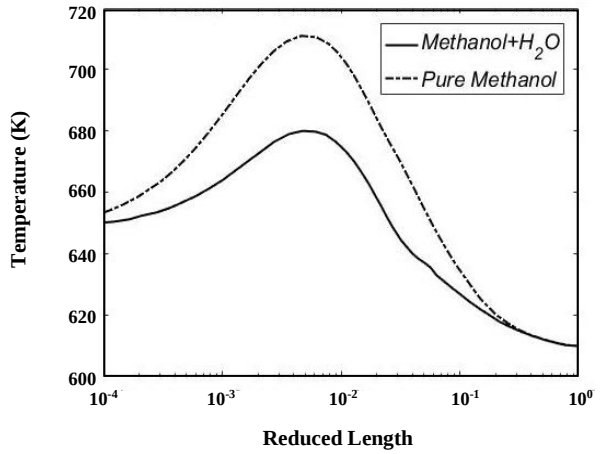

Fig. 7: Temperature profile for - . inlet pure methanol and — inlet methanol+water.

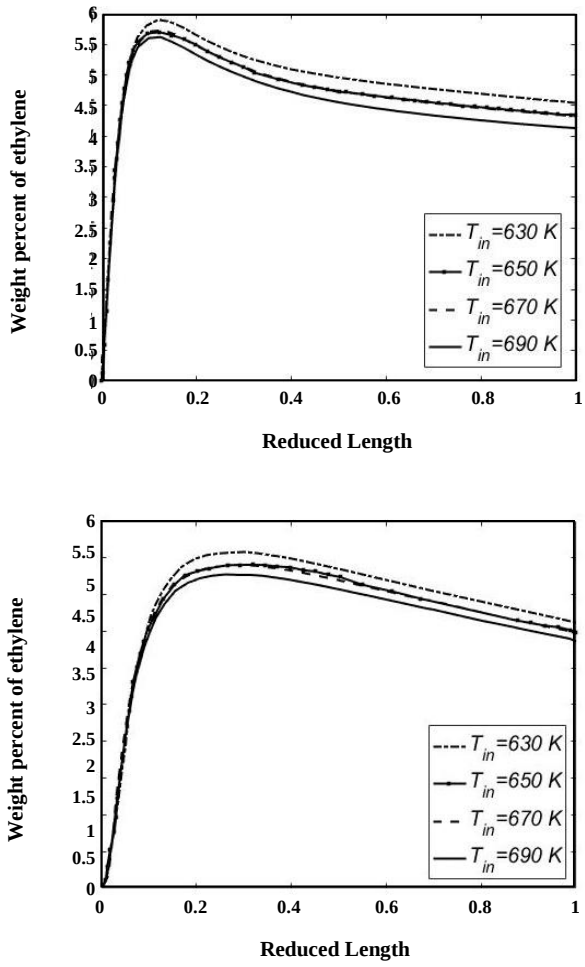

Fig. 8: Concentration profiles of products along the reactor for different inlet temperatures, (a) ethylene, (b) propylene.

of decreasing methanol content of the feed and high specific heat capacity of water. Considering benefits of adding water at reactor inlet, influence of other parameters on reactor performance will be discussed in the case of injecting water and methanol together into the reactor.

Effect of inlet temperature on reactor performance

Besides the main reaction, there are many other reactions taking place inside the reactor and producing different byproducts. So, the temperature should be optimized in such a way that favors the main reaction. Fig. 8 (a) and (b) illustrate concentration profiles of the main products (ethylene and propylene) within the reactor with respect to inlet temperature. As can be seen, increasing inlet temperature causes main products to decrease slightly because the main reaction is exothermic and temperature increase shifts main reaction to the left. However, at low temperatures the rate of the main reaction decreases sharply. As it is illustrated in Fig. 9 the maximum temperature within the reactor increases with increase of inlet temperature and also its location moves towards the inlet of the reactor. The results at outlet of the reactor demonstrate that fixed-bed reactor is not highly sensitive to changes in inlet temperature. This is one of the most important advantages of this type of reactors. According to Fig. 9, the best value for inlet temperature was selected as 650K between other assessed values in this research. In this temperature, the main reactions will take place at good speed while generation of hot spot within the reactor is prevented.

Effect of electrical resistance furnace temperature on reactor performance

Fig. 10 illustrates the effect of electrical resistance temperature on ethylene and propylene weight percent at reactor outlet when inlet temperature was 650K. As can be seen, furnace temperature strongly affects product yield. Thus, it can be chosen as manipulating variable for process control. As shown in Fig. 10, there is an optimal value within tested electrical resistance temperature range for maximizing main product concentration.

Structure of control system

Because MTO process is usually performed in a non-adiabatic fixed-bed reactor, control of maximum

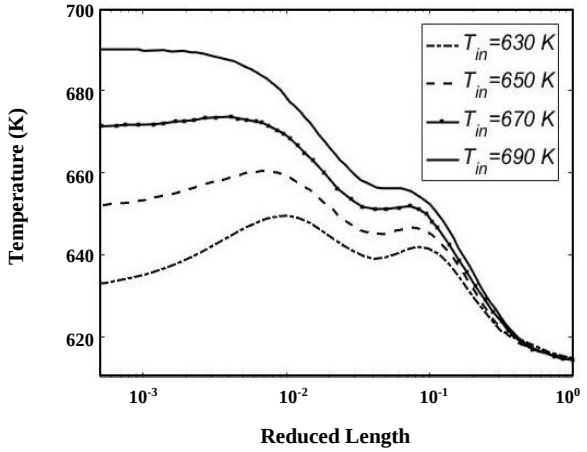

Fig. 9: Temperature profile along the reactor for different inlet temperatures.

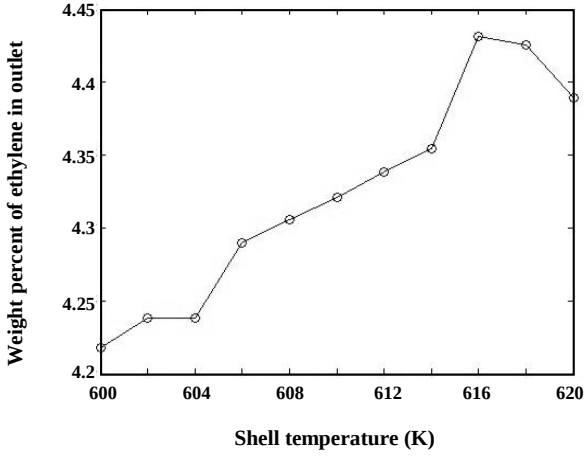

Fig. 10: Ethylene weight percent at the reactor outlet with respect to different furnace temperatures.

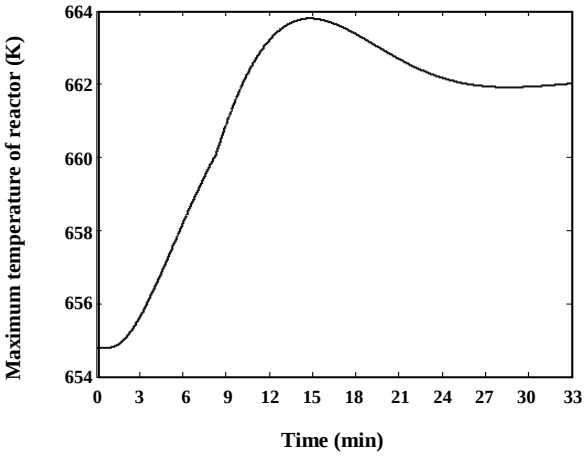

Fig. 11: Response of the maximum temperature within the reactor to a +20 ºC step change on electrical resistance temperature.

temperature inside the reactor is very important in order to avoid catalyst deactivation at high temperatures. Thus, signal of maximum temperature measurement inside the reactor must be sent to a temperature controller to control the maximum temperature by manipulating electrical resistance furnace temperature which was found as the most affecting parameter. In this work PID and NNMP controllers were investigated for process control and their performances were compared to each other.

PID controller

In order to design a controller for the process, the relationship between maximum temperature inside the reactor and electrical resistance temperature was modeled using open loop response. For this purpose, a step change of +20 ˚C on steady-state value of electrical resistance temperature was applied.

According to Fig. 11, response of maximum temperature can be approximated by a second order with time delay model whose calculated parameters are shown in Table 5.

Internal Model Control (IMC) technique was used for tuning the parameters of PID controller [59]. In this method parameters of PID controller are calculated using the following equations:

$$G_c(s) = K_c\left(1+\frac{1}{\tau_I s}+\tau_D s\right), \text{ PID Controller transfer function} \quad (10)$$

$$K_c = \frac{2\tau\zeta}{K_p\left(\tau_c+\tau_d\right)} \quad (11)$$

$$\tau_I = 2\tau\zeta \quad (12)$$

$$\tau_D = \frac{\tau^2}{2\tau\zeta} \quad (13)$$

where τ_c is a tuning parameter and is obtained by minimizing integral of square of errors for set point tracking. Calculated PID parameters are given in Table 6.

Set point tracking

Set point tracking capability of the designed control system was assessed by applying 8 ˚C step change on the set point of maximum temperature inside the reactor. Fig. 12 shows the response of the system for this step change.

Table 5: Approximated input-output relationship between maximum temperature within the reactor and electrical resistance furnace temperature.

K_p	0.362
τ (s)	240.6
ζ	0.41
τ_d (s)	33.9

Table 6: Parameters of designed PID controller.

K_c	8.25
τ_I (s)	197.18
τ_D (s)	293.62
τ_c (s)	32.17

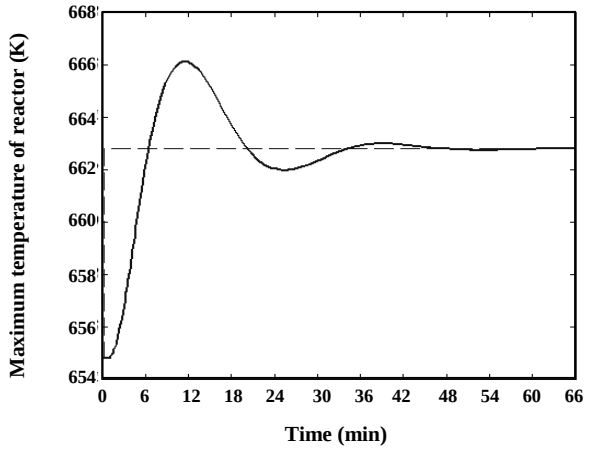

Fig. 12: Performance of the control system due to a step-change on reactor maximum temperature set-point.

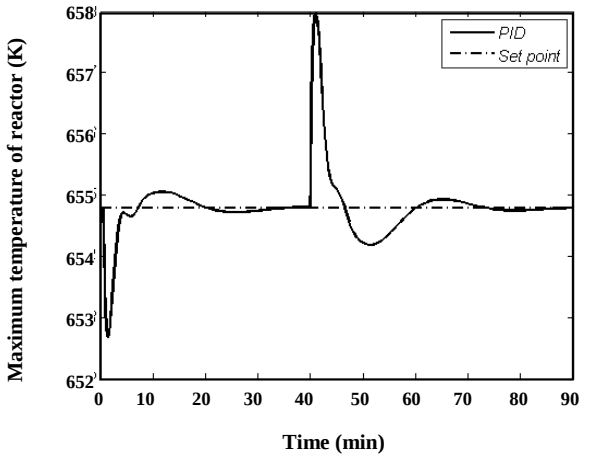

Fig. 13: Response of maximum temperature inside the reactor for disturbance rejection applied on feed composition.

As can be seen, the maximum temperature approaches to the new set point value with acceptable speed and oscillations.

Disturbance rejection

To observe the performance of proposed control structure and PID controller for disturbance rejection, a step change on feed composition was applied. The information of feed disturbance is presented in Table 7. Closed loop response of the system for this disturbance is shown in Fig. 13. Simulation results showed that the controller works well for disturbance rejection.

ANN controller

To control the process using ANN controller, Neural Network Model Predictive (NNMP) control method was used. Activation function for all neurons in the network was hyperbolic tangent and training algorithm was Levenberg-Marquardt. Optimum number of neurons in hidden layer was obtained as 6 using trial and error. A total of 100 input-output data set with time intervals of 60s was obtained by applying random changes on furnace temperature within the range of 600 to 645K. The simulation results are shown in Fig. 14.

The generated data was used for training of NNMP controller and then the trained network was used for the control of fixed-bed reactor. The parameters of optimization module are shown in Table 8.

Set point tracking

Set point tracking capability of trained NNMP controller was investigated by applying a step change on set point of maximum temperature inside the reactor. Fig. 15 indicates the results showing favorable performance of ANN controller. For clarity, the response of control system with PID controller is also shown on the figure. The response of control system with NNMPC represents a small offset because it doesn't have any integrator and acts similar to a PD controller, while PID controller has an integrator and won't have any offset.

Table 9 compares closed-loop responses of PID and NNMP controllers for set-point tracking. As it is evident, PID controller has smaller rise time and settling time, while NNMP controller responds with smaller overshoot and has a small offset of about 1 K.

Table 7: Specifications of disturbance in feed composition.

Component	Weight percent at t<0	Weight percent at t=0.5 min	Weight percent at t=40 min
CH_3OH	75	70	77.5
H_2O	25	30	27.5

Table 8: Parameters of optimization module of NNMP controller used in this study.

Sampling time (s)	Prediction horizon	Control horizon
1	8	2

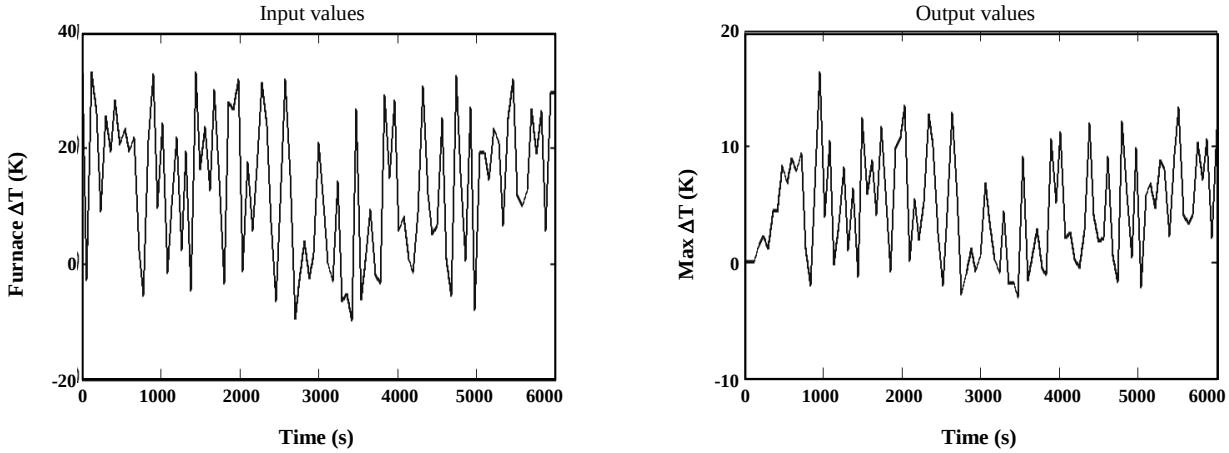

Fig. 14: Input-output data generated by simulation and used for training NNMPC.

Disturbance rejection

NNMP controller was used for rejection of disturbance described in Table 7 whose results are shown in Fig. 16. For comparison, results of disturbance rejection using PID controller are also shown on the figure. As can be seen, NNMPC hasn't been able to remove disturbance completely while PID has removed it. But, NNMPC has a smaller response time for first applied disturbance and smaller overshoot compared to the response of PID controller.

CONCLUSIONS

In this paper, modeling, simulation and control of a Methanol-To-Olefins (MTO) laboratory fixed-bed reactor with electrical resistance furnace was investigated in both steady-state and dynamic conditions. At steady-state the effect of three parameters including feed composition, inlet temperature and electrical resistance furnace temperature on reactor performance was studied. Then, after investigating dynamic behavior of the reactor by dynamic simulation, a control system was designed for the control of the reactor based on the open-loop response of the processing system. PID and NNMP controllers were used for process control and their performances were compared to each other. Results of this work can be abstracted as follows:

1. The kinetic model used in this study gives a good approximation of reactor performance.

2. Simulation results showed that the rates of exothermic reactions at beginning of the reactor are very high and main products are produced in this section.

3. Increasing inlet composition of water, decreased maximum temperature inside the reactor.

4. Increasing inlet temperature caused slight reduction of main products namely ethylene and propylene.

5. Location of maximum temperature inside the reactor moved towards the inlet of the reactor as the inlet temperature increased.

6. PID controller had smaller rise time, larger overshoot and faster response compared to NNMPC with

Table 9: Comparison of closed loop response of PID and NNMP controllers for set-point tracking.

Dynamic characteristic	PID controller	NNMP controller
Offset (K)	0	1
Rise time (min)	6.28	10.83
Overshoot (%)	41.67	29.91
Peak response time (min)	11.58	16.83
Settling time (min)	29.75	33

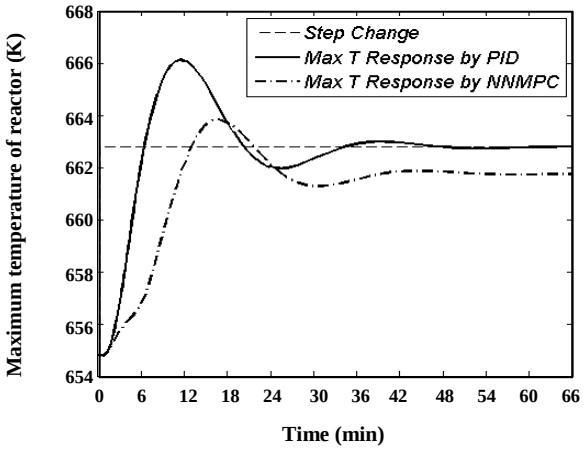

Fig. 15: Set-point tracking of closed-loop system for control of maximum temperature inside the reactor using PID and NNMP controllers.

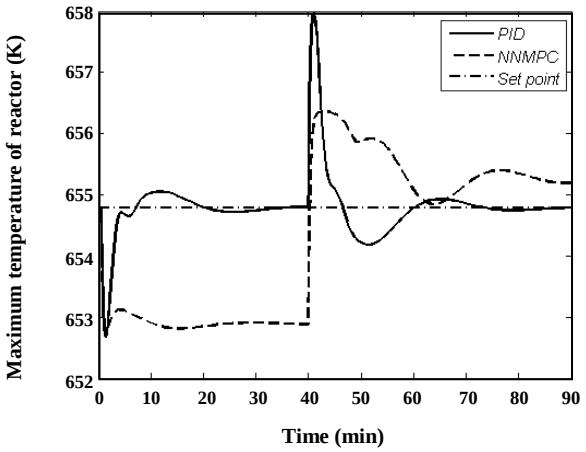

Fig. 16: Feed composition disturbance rejection of closed-loop system for control of maximum temperature inside the reactor using PID and NNMP controllers.

no offset, while NNMPC had smaller overshoot and offset was about 1 K for set-point tracking. Also, tuning of PID controller is easier and its response has no offset.

Symbols

A	Cross sectional area of the reactor, m^2
C_i	Concentration of ith chemical species, $kmol/m^3$
C_{pi}^{ig}	Ideal gas heat capacity of ith chemical species, J/kmol.K
$C_{pcat.}$	Heat capacity of catalyst, J/kmol.K
d	Reactor diameter, m
d_p	Average diameter of catalyst particles, m
E_j	Activation energy of jth reaction, J/kmol
F_i	Molar flow rate of ith chemical species, kmol/s
ΔH_j	Heat of reaction of jth chemical reaction, J/kmol
K_p	Process gain
k_j	Reaction rate constant for jth reaction
k_{j0}	Pre-exponential term in Arrhenius equation for jth reaction
m	Number of reactions, equals to 53
m_s	Number of chemical species including intermediates, equals to 36
r_i	Rate of production of ith chemical species, kmol/(m^3 of catalyst).s
R	Universal gas constant, 8314 J/kmol.K
R_j	Rate of jth chemical reaction, kmol/(m^3 of catalyst).s
R_M	Logarithmic mean radius, m
T	Reactor temperature, K
T_a	Electrical resistance furnace temperature, K
T_{aref}	Reference value for electrical resistance furnace temperature, K
u	Superficial gas velocity, m/s
U	Overall heat transfer coefficient, $J/m^2.s.K$
z	Axial coordinate, m

Greek Symbols

$\alpha_{conv.}$	Convective heat transfer coefficient, J/m^2.s.K
α_{ra}	Radiative heat transfer coefficient through gas layer, J/m^2.s.K
$\alpha_{W,eff}$	Effective wall heat transfer coefficient, J/m^2.s.K
δ	Glass wall thickness, m
ε	Void fraction
η	Effectiveness factor
λ_{eff}	Radial effective conductivity of the bed, J/m^2.s.K
λ_W	Wall conductivity, J/m^2.s.K
μ_g	Gas viscosity, kg/m.s
v_{ij}	Stoichiometric coefficient of ith chemical species in jth chemical reaction
ρ_g	Gas density, kg/m^3
$\rho_{cat.}$	Catalyst density, kg/m^3
τ	Time constant of the process, s
τ_d	Time delay, s
ζ	Damping ratio

Appendix A

Reaction network for MTO process proposed by [19] with some modifications for abstraction

Methanol reactions:

$$CH_3OH \longrightarrow CO + 2H_2$$

$$2CH_3OH \rightleftharpoons CH_3OCH_3 + H_2O$$

$$CH_3OCH_3 \rightleftharpoons 2{:}CH_2 + H_2O$$

Light olefins formation:

$$:CH_2 + CH_3OH \rightleftharpoons C_2H_4 + H_2O$$

$$:CH_2 + CH_3OCH_3 \rightleftharpoons C_2H_4 + CH_3OH$$

$$:CH_2 + CH_3OCH_3 \rightleftharpoons C_3H_6 + H_2O$$

Higher olefins formation:

$$:CH_2 + C_nH_{2n} \longrightarrow C_{n+1}H_{2n+2} \qquad n = 2,3,4,5,6$$

Methane formation:

$$:CH_2 + H_2 \longrightarrow CH_4$$

Carbenium ions formation from olefins:

$$C_2H_{2n} \underset{-A^-}{\overset{+A^-H^+}{\rightleftharpoons}} C_n^+H_{2n+1} \qquad n = 2,\ldots,5$$

Higher Olefins Formation by Carbenium ions:

$$C_n^+H_{2n+1} + C_3H_6 \xrightarrow[-A^-H^+]{+A^-} C_{2n}H_{4n} \qquad n = 3,4$$

$$C_n^+H_{2n+1} + C_2H_4 \xrightarrow[-A^-H^+]{+A^-} C_{n+2}H_{2n+4} \qquad n = 4,5$$

Paraffins formation:

$$C_n^+H_{2n+1} + C_mH_{2m} \xrightarrow[-A^-H^+]{+A^-} C_{n+2}H_{2n+2} + C_mH_{2m-2}$$

$$n = 3,4,5 \quad , \quad m = 6,7$$

Cyclodienes formation:

$$C_n^+H_{2n+1} + C_mH_{2m-4} \xrightarrow[-A^-H^+]{+A^-} C_nH_{2n+2} + C_mH_{2m-4}$$

$$n = 3,4,5 \quad , \quad m = 6,7$$

Aromatics formation:

$$C_n^+H_{2n+1} + C_mH_{2m-4} \xrightarrow[-A^-H^+]{+A^-} C_nH_{2n+2} + C_mH_{2m-6}$$

$$n = 3,4,5 \quad , \quad m = 6,7$$

Aromatics condensation:

$$2C_6H_6 \longrightarrow C_{10}H_8 + C_2H_4$$

$$2C_6H_6 \longrightarrow C_9H_8 + C_2H_4 + C$$

Aromatics alkylation:

$$CH_3OH + C_nH_{2n-6} \longrightarrow C_{n+1}H_{2n-4} + H_2O \ , \ n = 6,\ldots 11$$

$$CH_3OH + C_nH_{2n-12} \longrightarrow C_{n+1}H_{2n-10} + H_2O \ , \ n = 10,11$$

Paraffins demethanization:

$$C_nH_{2n+2} \longrightarrow C_{n-1}H_{2n-2} + CH_4 \quad , \quad n = 5,4,3$$

Received : May 30, 2014 ; Accepted : Apr. 10, 2017

REFERENCES

[1] Van V., "Methanol To Olefins", SRI, Process Economics Report Number 261 (2007).

[2] Xiang D., Qian Y., Man Y., Yang S., Techno-Economic Analysis of the Coal-to-Olefins Process in Comparison with the Oil-to-Olefins Process, *Appl. Energy*, **113**: 639-647 (2014).

[3] Stöcker M., Methanol-to-Hydrocarbons: Catalytic Materials and Their Behavior, *Microporous Mesoporous Mater.*, **29** (1–2): 3-48 (1999).

[4] Al Wahabi S.M., "Conversion of Methanol to Light Olefins on SAPO-34: Kinetic Modeling and Reactor Design", PhD. Thesis, Texas A&M University (2003).

[5] Froment G.F., Dehertog W.J.H., Marchi A.J., Zeolite Catalysis in the Conversion of Methanol into Olefins, In: "Catalysis", J.J. Spivey (Ed.), The Royal Society of Chemistry, 1-64 (1992).

[6] Freiding J., Kraushaar-Czarnetzki B., Novel Extruded Fixed-Bed MTO Catalysts with High Olefin Selectivity and High Resistance Against Coke Deactivation, *Appl. Catal., A*, **391** (1–2): 254-260 (2011).

[7] Yang H., Liu Z., Gao H., Xie Z., Synthesis and Catalytic Performances of Hierarchical SAPO-34 Monolith, *J. Mater. Chem.*, **20**(16): 3227-3231 (2010).

[8] Emrani P., Fatemi S., Ashraf-Talesh S., Effect of Synthesis Parameters on Phase Purity, Crystallinity and Particle Size of SAPO-34, *Iran. J. Chem. Chem. Eng. (IJCCE)*, **30** (4): 29-36 (2011).

[9] Chang C.D., Hydrocarbons from Methanol, *Catal. Rev.*, **25** (1): 1-118 (1983).

[10] Chen D., Rebo H.P., Moljord K., Holmen A., Methanol Conversion to Light Olefins over SAPO-34. Sorption, Diffusion, and Catalytic Reactions, *Ind. Eng. Chem. Res.*, **38** (11): 4241-4249 (1999).

[11] Haw J.F., Song W., Marcus D.M., Nicholas J.B., The Mechanism of Methanol to Hydrocarbon Catalysis, *Acc. Chem. Res.*, **36** (5): 317-326 (2003).

[12] Wu W., Guo W., Xiao W., Luo M., Methanol Conversion to Olefins (MTO) Over H-ZSM-5: Evidence of Product Distribution Governed by Methanol Conversion, *Fuel Process. Technol.*, **108**: 19-24 (2013).

[13] Bos A.N.R., Tromp P.J.J., Akse H.N., Conversion of Methanol to Lower Olefins. Kinetic Modeling, Reactor Simulation, and Selection, *Ind. Eng. Chem. Res.*, **34** (11): 3808-3816 (1995).

[14] Gayubo A.G., Aguayo A.T., Olazar M., Vivanco R., Bilbao J., Kinetics of the Irreversible Deactivation of the HZSM-5 Catalyst in the MTO Process, *Chem. Eng. Sci.*, **58** (23–24): 5239-5249 (2003).

[15] Park T.-Y., Froment G.F., Kinetic Modeling of the Methanol to Olefins Process. 1. Model Formulation, *Ind. Eng. Chem. Res.*, **40** (20): 4172-4186 (2001).

[16] Park T.-Y., Froment G.F., Kinetic Modeling of the Methanol to Olefins Process. 2. Experimental Results, Model Discrimination, and Parameter Estimation, *Ind. Eng. Chem. Res.*, **40** (20): 4187-4196 (2001).

[17] Alwahabi S.M., Froment G.F., Single Event Kinetic Modeling of the Methanol-to-Olefins Process on SAPO-34, *Ind. Eng. Chem. Res.*, **43** (17): 5098-5111 (2004).

[18] Chen D., Grønvold A., Moljord K., Holmen A., Methanol Conversion to Light Olefins over SAPO-34: Reaction Network and Deactivation Kinetics, *Ind. Eng. Chem. Res.*, **46** (12): 4116-4123 (2007).

[19] Mihail R., Straja S., Maria G., Musca G., Pop G., A Kinetic Model for Methanol Conversion to Hydrocarbons, *Chem. Eng. Sci.*, **38** (9): 1581-1591 (1983).

[20] Rostami R.B., Lemraski A.S., Ghavipour M., Behbahani R.M., Shahraki B.H., Hamule T., Kinetic Modelling of Methanol Conversion to Light Olefins Process Over Slicoaluminophosphate (SAPO-34) Catalyst, *Chem. Eng. Res. Des.*, **106**: 347-355 (2016).

[21] Kaarsholm M., Rafii B., Joensen F., Cenni R., Chaouki J., Patience G.S., Kinetic Modeling of Methanol-to-Olefin Reaction over ZSM-5 in Fluid Bed, *Ind. Eng. Chem. Res.*, **49**: 29-38 (2010).

[22] Gayubo A.G., Arandes J.M., Aguayo A.T., Olazar M., Bilbao J., Calculation of the Kinetics of Deactivation by Coke in an Integral Reactor for a Triangular Scheme Reaction, *Chem. Eng. Sci.*, **48** (6): 1077-1087 (1993).

[23] Chen D., Rebo H.P., Grønvold A., Moljord K., Holmen A., Methanol Conversion to Light Olefins Over SAPO-34: Kinetic Modeling of Coke Formation, *Microporous Mesoporous Mater.*, **35–36** (0): 121-135 (2000).

[24] Kaarsholm M., Joensen F., Nerlov J., Cenni R., Chaouki J., Patience G.S., Phosphorous Modified ZSM-5: Deactivation and Product Distribution for MTO, *Chem. Eng. Sci.*, **62** (18–20): 5527-5532 (2007).

[25] Chae H.-J., Song Y.-H., Jeong K.-E., Kim C.-U., Jeong S.-Y., Physicochemical Characteristics of ZSM-5/SAPO-34 Composite Catalyst for MTO Reaction, *J. Phys. Chem. Solids*, **71** (4): 600-603 (2010).

[26] Lee Y.J., Lee J.S., Park Y.S., Yoon K.B., Synthesis of Large Monolithic Zeolite Foams with Variable Macropore Architectures, *Adv. Mater.*, **13** (16): 1259-1263 (2001).

[27] Müller S., Liu Y., Vishnuvarthan M., Sun X., van Veen A.C., Haller G.L., Sanchez-Sanchez M., Lercher J.A., Coke Formation and Deactivation Pathways on H-ZSM-5 in the Conversion of Methanol to Olefins, *J. Catal.*, **325**: 48-59 (2015).

[28] Chen J.Q., Bozzano A., Glover B., Fuglerud T., Kvisle, S., Recent Advancements in Ethylene and Propylene Production Using the UOP/Hydro MTO Process, *Catal. Today*, **106** (1–4): 103-107 (2005).

[29] Chang C.D., Kuo J.C.W., Lang W.H., Jacob S.M., Wise J.J., Silvestri A.J., Process Studies on the Conversion of Methanol to Gasoline, *Ind. Eng. Chem. Process Des. Dev.*, **17** (3): 255-260 (1978).

[30] Anderson J.R., Mole T., Christov V., Mechanism of Some Conversions Over ZSM-5 Catalyst, *J. Catal.*, **61** (2): 477-484 (1980).

[31] Voltz S.E., Wise J.J., "Development Studies on Conversion of Methanol and Related Oxygenates to Gasoline", Final Report, US ERDA Contract No. E (49-18)-1773 (1976).

[32] Gayubo A.G., Aguayo A.T., Sánchez del Campo A.E., Tarrío A.M., Bilbao J., Kinetic Modeling of Methanol Transformation into Olefins on a SAPO-34 Catalyst, *Ind. Eng. Chem. Res.*, **39** (2): 292-300 (2000).

[33] Chen N.Y., Reagan W.J., Evidence of Autocatalysis in Methanol to Hydrocarbon Reactions over Zeolite Catalysts, *J. Catal.*, **59** (1): 123-129 (1979).

[34] Chang C.D., A Kinetic Model for Methanol Conversion to Hydrocarbons, *Chem. Eng. Sci.*, **35**(3): 619-622 (1980).

[35] Alwahabi S.M., Froment G.F., Conceptual Reactor Design for the Methanol-to-Olefins Process on SAPO-34, *Ind. Eng. Chem. Res.*, **43** (17): 5112-5122 (2004).

[36] Nijemeisland M., Dixon A.G., CFD Study of Fluid Flow and Wall Heat transfer in a Fixed Bed of Spheres, *AIChE J.*, 50 (5): 906-921 (2004).

[37] Zhuang Y.-Q., Gao X., Zhu Y.-p., Luo Z.-h., CFD Modeling of Methanol to Olefins Process in a Fixed-Bed Reactor, *Powder Technol.*, **221**: 419-430 (2012).

[38] Schoenfelder H., Hinderer J., Werther J., Keil F.J., Methanol to Olefins—Prediction of the Performance of a Circulating Fluidized-Bed Reactor on the Basis of Kinetic Experiments in a Fixed-Bed Reactor, *Chem. Eng. Sci.*, **49** (24, Part 2): 5377-5390 (1994).

[39] Soundararajan S., Dalai A.K., Berruti F., Modeling of Methanol to Olefins (MTO) Process in a Circulating Fluidized Bed Reactor, *Fuel*, **80** (8): 1187-1197 (2001).

[40] Chang J., Zhang K., Chen H., Yang Y., Zhang L., CFD Modelling of the Hydrodynamics and Kinetic Reactions in a Fluidised-Bed MTO Reactor, *Chem. Eng. Res. Des.*, **91** (12): 2355-2368 (2013).

[41] Lu B., Luo H., Li H., Wang W., Ye M., Liu Z., Li J., Speeding up CFD Simulation of Fluidized Bed Reactor for MTO by Coupling CRE Model, *Chem. Eng. Sci.*, **143**: 341-350 (2016).

[42] Green D.W., Perry R.H., "Perry's Chemical Engineers' Handbook", McGraw-Hill Book Company, New York, USA (2007).

[43] Hottel A.F., Sarofim H.C., "Radiative Transfer", McGraw-Hill Book Company, New York, USA (1967).

[44] Froment G.F., Fixed Bed Catalytic Reactors—Current Design Status, *Ind. Eng. Chem.*, **59** (2): 18-27 (1967).

[45] de Wasch A.P., Froment G.F., Heat Transfer in Packed Beds, *Chem. Eng. Sci.*, **27** (3): 567-576 (1972).

[46] Dixon A.G., Cresswell D.L., Theoretical Prediction of Effective Heat Transfer Parameters in Packed Beds, *AIChE J.*, **25** (4): 663-676 (1979).

[47] Froment G.F., Bischoff K.B., De Wilde J., "Chemical Reactor Analysis and Design", Wiley, New York, USA (2011).

[48] Schiesser W.E., "The Numerical Method of Lines: Integration of Partial Differential Equations", Academic Press, Inc., San Diego, California (1991).

[49] Samarasinghe, S., "Neural Networks for Applied Sciences and Engineering: From Fundamentals to Complex Pattern Recognition", Auerbach Publications, Taylor & Francis Group, New York (2006).

[50] Krose B., van der Smagt P., "An Introduction to Neural Networks ", The University of Amsterdam, The Netherlands (1996).

[51] Valadkhani A., Shahrokhi M., Simulation and Control of an Aromatic Distillation Column, *Iran. J. Chem. Chem. Eng. (IJCCE)*, **26**(2): 97-108 (2007).

[52] Åkesson B.M., Toivonen H.T., A Neural Network Model Predictive Controller, *J. Process Control*, **16**(9): 937-946 (2006).

[53] Draeger A., Engell S., Ranke H., Model Predictive Control Using Neural Networks, *IEEE Control Syst.*, **15**(5): 61-66 (1995).

[54] Yeh T.-M., Huang M.-C., Huang C.-T., Estimate of Process Compositions and Plantwide Control from Multiple Secondary Measurements Using Artificial Neural Networks, *Comput. Chem. Eng.*, **27** (1): 55-72 (2003).

[55] Akpan V.A., Hassapis G.D., Nonlinear Model Identification and Adaptive Model Predictive Control Using Neural Networks, *ISA Trans.*, 50 (2): 177-194 (2011).

[56] Yu D.L., Gomm J.B., Implementation of Neural Network Predictive Control to a Multivariable Chemical Reactor, *Control Eng. Pract.*, **11**(11): 1315-1323 (2003).

[57] Kittisupakorn P., Thitiyasook P., Hussain M.A., Daosud W., Neural Network Based Model Predictive Control for a Steel Pickling Process, *J. Process Control*, **19** (4): 579-590 (2009).

[58] Shampine, L. F., and Reichelt, M. W., The MATLAB ODE Suite, *SIAM J. Sci. Comput.*, 18: 1-22 (1997).

[59] Tan W., Liu J., Chen T., Marquez H.J., Comparison of Some Well-Known PID Tuning Formulas, *Comput. Chem. Eng.*, **30** (9): 1416-1423 (2006).